Cement and Concrete Research 40 (2010) 1386–1392

Contents lists available at ScienceDirect

Cement and Concrete Research

journal homepage: http://ees.elsevier.com/CEMCON/default.asp

Pore solution composition and alkali diffusion in inorganic polymer cement

Redmond R. Lloyd, John L. Provis *, Jannie S.J. van Deventer

Department of Chemical & Biomolecular Engineering, University of Melbourne, Victoria 3010, Australia

ARTICLE INFO

Article history:
Received 13 October 2009
Accepted 28 April 2010

Keywords:
Inorganic polymer
Geopolymer
Aluminosilicate
Pore solution (B)
Durability (C)
Alkali (D)

ABSTRACT

Extraction of pore solutions from hardened inorganic polymer cement ("geopolymer") paste samples shows that the pore network of these materials is rich in alkali cations and has pH>13, with a relatively low dissolved Si concentration. However, there is little soluble Ca available in these materials to play a buffering role similar to $Ca(OH)_2$ or high-Ca C–S–H in hydrated Portland cements, meaning that preventing alkali loss is essential in ensuring the protection of reinforcing steel. It has been seen previously that calcium in an inorganic polymer cement binder is important in the formation of a low-permeability pore system; alkali diffusion measurements confirm these observations and highlight the role of Ca in reducing effective alkali diffusion coefficients by up to an order of magnitude. This is crucial for the durability of inorganic polymer concretes containing steel reinforcement, as it appears that the use of calcium-containing raw materials will be highly preferable.

1. Introduction

One of the important aspects of the pore system of intact Portland cement concrete is its high pH, typically around 13–14. This elevated pH develops initially due to the effect of alkalis contained in the cement, and is buffered at high alkalinity (pH>12) in undamaged pastes by saturation of the pore solution with respect to $Ca(OH)_2$, a product of the hydration of tri- and di-calcium silicates. The high pH of the pore solution ensures the stability of the phases present in hydrated Portland cement. In structural concrete the pore solution performs an even more important protective function, by causing a passive film to form on the surface of embedded steel reinforcement. A loss of alkalinity from reinforced concrete leads to depassivation and corrosion of embedded steel; corrosion commences as the pH falls below about 9.5, the passive film on the steel surface disappears at pH 8 and catastrophic corrosion occurs at any pH below 7 [1]. Corrosion of the steel results in the formation of iron oxides, resulting in expansion and leading ultimately to failure of the concrete [2].

Inorganic polymer cement (IPC), also known as 'geopolymer' [3,4], is a class of material obtained by the reaction of an aluminosilicate source (most commonly fly ash and/or metallurgical slags) with an alkali hydroxide or silicate solution. The reaction product is a highly cross-linked aluminosilicate gel, which provides mechanical performance comparable to hardened hydrated Portland cement but with a smaller Greenhouse footprint [5]. It has therefore been widely proposed that IPC will find use as an alternative to Portland cement in a variety of structural and non-structural applications, and its commercial utilisation has commenced in Australia and other parts of the world.

However, before IPC can be confidently used with embedded steel reinforcement in structural elements, it is important to establish that the pore solution is sufficiently alkaline to passivate the steel. Prominent among the very few published studies of the corrosion of reinforcing in fly ash-derived IPC is the work of Palomo and colleagues [6–8], who used electrochemical techniques to establish that embedded steel is indeed protected in alkali-activated fly ash mortars. Their initial conclusion [6] was that there is "no cause to fear that corrosion may limit the durability of reinforced concrete structures built with these new types of activated fly ash cement". However, such a conclusion may appear premature on the basis of a limited number of IPC formulations tested, all of which were activated with quite high alkali concentrations (*i.e.* 8–10 M NaOH), and little or no added soluble silica. It would be expected that lower alkali content — as is considered desirable in commercial IPC mixes due to both the relatively high cost of NaOH and the severe efflorescence often observed at high NaOH content — would result in reduced pore solution alkalinity and potentially less successful passivation of the steel. The longer-duration tests conducted by Fernández-Jiménez et al. [8] showed an enhancement of durability by the addition of some soluble silica to the activating solution, attributed by those authors to the slower carbonation of these samples than their NaOH-activated counterparts.

Additionally, it is critical to determine the ability of the IPC to maintain steel passivity in service. The ability to protect steel can be lost, due either to loss of alkalinity or to the ingress of other species such as chlorides. Establishing that the pore solution of IPC is able to passivate steel is therefore only part of the answer; the ability of the cement to retain its alkalinity and resist the ingress of other ions is

* Corresponding author. Tel.: +61 3 8344 8755; fax: +61 3 8344 4153.
E-mail address: jprovis@unimelb.edu.au (J.L. Provis).

0008-8846/$ – see front matter © 2010 Elsevier Ltd. All rights reserved.
doi:10.1016/j.cemconres.2010.04.008

critically important. This depends most critically on permeability, which depends in turn on porosity and pore network structure. The pore structure of IPC has recently been shown to be highly complex, and also critically dependent on binder chemistry [9], and this must be taken into consideration in any discussion of durability.

Characterisation of IPC pore solutions will therefore comprise the first part of this paper. The remainder of the paper involves characterisation of some functional aspects of the pore system of IPC, specifically the pore solution alkalinity and the rate at which alkali can diffuse from the paste. In many ways these are more important than measurements of porosity or pore size distribution, as they provide a direct indication of the likely durability of inorganic polymer concretes.

2. Materials and methods

2.1. Sample synthesis

Sample synthesis and curing were carried out as described by Lloyd et al. [10]. Briefly, fly ashes were sourced from Gladstone power station, Queensland, Australia (GFA; class F according to ASTM C618; supplied by Pozzolanic Industries), Port Augusta power station, South Australia, Australia (PAFA; also class F; Adelaide Brighton Cement), and Huntly Power Station, New Zealand (HFA; class C; Golden Bay Cement). Ground granulated blast-furnace slag (GGBS) was supplied by Independent Cement and Lime, Australia. The oxide compositions of all solid raw materials are given in Table 1. X-ray diffractometry [11] showed some mullite, quartz and minor iron oxides in all ashes, and larnite in the high-calcium HFA. No crystalline phases were observed in the GGBS.

The activating solutions were formulated by blending sodium silicate solution (Grade N, PQ Australia) with sodium hydroxide solution (50 wt.%, Aldrich) and reverse osmosis (RO) grade deionised water, providing 7 wt.% SiO_2 and 7 wt.% Na_2O by mass of solid precursor unless specifically noted otherwise, which were mixed by hand with the fly ash and/or slag at water/binder (fly ash + slag) ratios of 0.325 for fly ash containing samples and 0.350 for samples containing slag only. Samples were cured in sealed moulds for 48 h at 65 °C (except those synthesised without dissolved silica in the activating solution, which required 80 °C to gain sufficient strength for demoulding after 48 h), then demoulded and aged at 23 °C for 90 days before testing.

2.2. Pore solution composition

The pore solution of IPC pastes was extracted following the technique described by Barneyback and Diamond [12]. Pressures of up to 500 MPa were used to express pore fluid from the samples being examined, with the pressure necessary to obtain a viable amount (approximately 1 mL) of pore solution varying according to the mechanical strength of the IPCs, with higher-strength samples requiring a higher pressure to extract the pore fluid. Extracted fluids were diluted immediately in Milli-Q water acidified to pH 1.0 with nitric acid and analysed for Na and K content by inductively coupled plasma-optical emission spectroscopy (ICP-OES). Analyses for calcium, aluminium and iron were also carried out, however the low concentrations of these elements (<1 mM in almost all cases) rendered the data imprecise. Silicon concentrations were also determined following dilution of the extracted pore solution in 0.2 M NaOH solution to avoid problems due to silica colloid formation during acidification; these data were also subject to a high degree of variability, but in all cases the silicon concentration was low (<10 mM).

Table 1
Oxide compositions of raw materials, in wt.%, from X-ray fluorescence analysis. LOI is loss on ignition at 1000 °C.

	GFA	PAFA	HFA	GGBS
Na_2O	0.28	3.23	1.05	0.26
MgO	1.35	2.11	2.06	6.02
Al_2O_3	27.84	30.10	18.10	13.18
SiO_2	45.46	48.16	47.49	32.88
P_2O_5	0.53	1.04	0.44	0.00
SO_3	0.21	0.09	1.01	3.50
K_2O	0.47	1.55	0.40	0.32
CaO	5.60	4.74	19.11	40.05
TiO_2	1.36	1.59	0.91	0.66
V_2O_5	0.00	0.05	0.03	0.03
MnO	0.19	0.05	0.03	0.40
Fe_2O_3	11.21	3.82	6.32	0.32
LOI	2.71	0.78	0.62	1.19

2.3. Diffusion of alkalis

Diffusion of alkali cations from IPC paste was examined by immersing IPC specimens in water and measuring the eluted cation concentration over time. One-dimensional diffusion conditions were attained by embedding discs of hardened IPC paste in epoxy resin (West 105, Ciba-Geigy, Australia). After curing the resin, each sample was sectioned using a low speed diamond saw to expose one face of the disc as shown in Fig. 1. Each sample was then immersed in 600 mL of RO water in a baffled vessel, and stirred at 100 rpm using an overhead stirrer. Each of the vessels was partially submerged in a water bath maintained at 23 °C. Samples were taken periodically and analysed by ICP-OES. At the conclusion of the experiment the sample was sectioned perpendicular to the original cut and the thickness of the paste disc measured using a calliper with 0.02 mm precision.

3. Results and discussion

3.1. Pore solution chemistry

The compositions of extracted pore solutions are presented in Table 2, grouped by the variable under examination. It is apparent that the pore solution of thermally cured IPC contains a high concentration of alkali metal cations; typically more than 500 mM and in several cases greater than 1 M. This is significantly higher than is observed in typical Portland cement paste, *ca.* 300 mM after an extended period [13], although this may vary considerably with the alkali content of the clinker [14]. Given the low concentration of aluminate and silicate counter-ions, it may be concluded that neutrality is maintained primarily by hydroxyl ions. This would provide the pore solution with a high pH, and indeed indicator paper showed the pH to be greater than 13 in all cases. Such a pH value would be expected to passivate steel reinforcement, and explains the good corrosion resistance generally observed in the literature [6–8].

Table 2 shows that the nature of the binder material has a very significant effect on the alkali concentration of the pore solution. As the calcium content of the binder increases (GFA ~ PAFA < HFA < GGBS), the amount of alkali present in the pore solution increases, indicating a

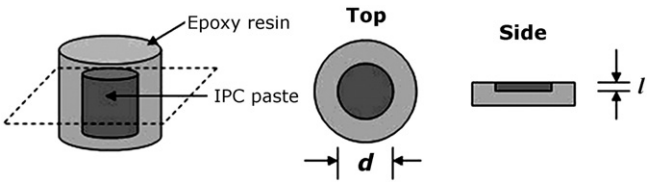

Fig. 1. Diagram of epoxy-embedded paste samples for alkali leaching. The diameter of the paste specimen, *d*, was 13.5 mm in all cases, and the thickness, *l*, between 3 and 5 mm.

Table 2
Na and K concentrations in pore solution expressed from cured IPC pastes. Sample formulations are presented as deviations from the 'base case': GFA-based paste, 7% SiO_2 and 7% Na_2O, water/binder 0.325, which is reproduced and shaded in grey in each sample series in which it is presented.

Parameter tested	Sample	[Na] (mM)	[K] (mM)
Binder type	GFA	612	2.7
	PAFA	782	15.2
	HFA	1567	14.9
	25% GGBS/75% GFA	711	10.9
	50% GGBS/50% GFA	973	10.6
	GGBS[a]	3617	77.1
Water/binder ratio	0.275	655	2.9
	0.325	612	2.7
	0.350	551	2.6
	0.375	446	2.2
Silicate content	4%	1227	14.3
(% by mass binder)	7%	612	2.7
	10%	451	2.1
Na_2O content	3%	658	3.4
(% by mass binder)	7%	612	2.7
	11%	1184	10.9
	15%	1499	18.0
Alkali type	Na	612	2.7
	50:50 (molar) Na:K	293	75.7
	K	22.2	243
Na_2O content	7%	217	1.4
(% by mass binder)	11%	348	1.9
(no soluble silicate)	15%	2069	12.7

[a] Water/binder ratio 0.350 required to enable mixing.

strong preference for incorporation of calcium over monovalent cations into the gel. The calcium concentration in the pore solution remains less than 1 mM in all samples.

One complicating factor in this analysis is the general decrease in aluminium content of the binder materials examined with increasing calcium content. It would be expected that tetrahedral aluminium would remove alkali cations from the pore solution and incorporate them into the gel, as has been previously observed for metakaolin-derived alkali aluminosilicate (geopolymer) gels [15,16] and for calcium aluminosilicate hydrate (C–A–S–H) gels [17]. The fly ash IPCs are predominantly X-ray amorphous alkali aluminosilicate gels [18], and although these display microstructural differences when compared with metakaolin-derived gels [11], the fundamental chemical motifs present are similar, and this will lead to similar alkali binding properties. IPCs derived from GGBS are usually dominated by C–A–S–H gels with some alkali substitution and/or binding [19–21]. Consequently, a decrease in the aluminium content of the binder would be expected to increase the amount of alkali remaining in the pore solution. However, the six-fold difference in pore solution alkali concentration between GFA and GGBS pastes cannot be solely accounted for by their relative aluminium contents, which are 28 wt.% and 13 wt.% Al_2O_3 respectively.

Puertas et al. [22] have previously activated Spanish blast-furnace slags with NaOH and Na silicate solutions to give 4% Na_2O in each case, and extracted the pore solutions by the same procedure used here at different times during the first 7 days of reaction. Those authors observed a decrease in pore solution [Na^+] and [Si] with time, with somewhat lower Na^+ concentrations than displayed by the GGBS sample in Table 2 (attributable mainly to the lower activator content of the sample), but higher [SiO_2] than observed here, as those samples were tested at younger ages. The lower Al concentration of the GGBS sample here (<1 mM, compared to ~5 mM and not notably decreasing with time in most of the samples in [22]) suggests that the use of a higher activator concentration enhances the incorporation of Al into the gel structure, as was also observed for pure C–S–H samples by Faucon et al. [23]. Song and Jennings [24] and Gruskovnjak et al. [25] did show Al concentrations decreasing over time in the pore solutions of GGBS activated by NaOH solutions and solid sodium metasilicate respectively. The dissolved Al concentrations in the investigation of Song and Jennings [24] all remained below ~1 mM for samples between 1 and 1000 h after mixing; Gruskovnjak et al. [25] observed concentrations as high as 7 mM at 1 day, decreasing to 3 mM after 180 days. However, neither study showed a particularly strong correlation between dissolved Al and Na concentrations.

A preference for incorporation of K over Na was also evident from the pore solution analyses, demonstrated by the substantially lower Na concentration in the sample activated by an equimolar Na–K activating solution. This effect has also been observed previously for metakaolin based geopolymers [26–28].

The effect of water-to-binder ratio on pore solution alkali content indicates no significant change in the extent or type of reaction over the range examined. The decrease in alkali concentration in the pore solution correlates with the dilution that would be expected as a result of higher water content. Similarly, the alkali content of the pore solution increases with the alkali content of the activating solution. The increase is approximately proportional, with the exception of samples at very low alkali content (3 wt.% Na_2O). As samples synthesised with low alkali content exhibited poor mechanical properties (they were weakly bound and friable), and have previously been observed to show a very low degree of binder formation by Wood's metal intrusion porosimetry [9], it is clear that little reaction of the fly ash was able to take place under these conditions.

The amount of dissolved silica initially present in the activating solution significantly affects the amount of alkali remaining in the pore solution. An inverse correlation was observed, indicating that higher silicate content led to a higher degree of reaction and thus less residual alkali. This correlates well with the theory advanced in previous work [10,18], in which dissolved silica in the activating solution enhances formation of the binder by preventing re-precipitation of dissolved species on to the surface of ash particles.

Samples activated without silicate showed low levels of residual alkali in the pore solution except when a very high alkali concentration was used. This indicates a high degree of reaction. This may be a function of the high curing temperature (80 °C) and extended curing time necessary to achieve acceptable mechanical strength for these samples. Other workers [29] have also observed a high extent of reaction for samples activated without sodium silicate when high-temperature curing for long duration was used. Because of the differences in curing, those samples cannot be compared directly with those activated with sodium silicate in this work.

3.2. The importance of portlandite

Due to the differences in reaction products of IPC and Portland cement it can be predicted that there will be significant differences in the properties of the pore solution. Perhaps the most important of these is the presence of calcium hydroxide (portlandite). Large amounts of calcium hydroxide are produced during hydration of calcium silicates in cement [30].

From the early stages of Portland cement hydration, that system is saturated with respect to $Ca(OH)_2$ [14]. Further accumulation of calcium results in precipitation of portlandite. Although generally considered an unfavourable reaction product as it has no cementitious value, portlandite provides the cement paste with a large reservoir of soluble Ca^{2+} and OH^- ions. Under conditions where the pore solution is leached from the paste (*e.g.* by exposure to flowing water) or neutralised (*e.g.* by exposure to carbon dioxide) the dissolution of portlandite allows the pH of the pore solution to be maintained for a long period. When the reservoir of portlandite is exhausted the pH of the pore solution drops and corrosion of reinforcing steel results, as shown in Fig. 2.

Unlike Portland cement (although like the high-volume supplementary cementitious material blends which are now in common use

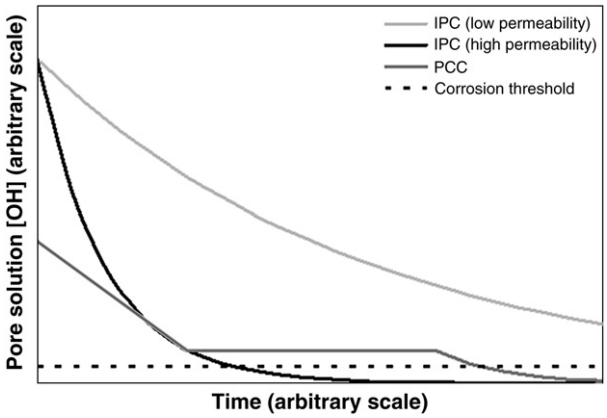

Fig. 2. Schematic of the pore solution hydroxide ion concentration within thin sections of IPC and Portland cement concrete (PCC) subject to leaching of the pore solution. The hydroxide ion content of the pore solution of PCC is maintained (after an initial period of decrease due to loss of the initial alkali content of the pores) due to replenishment of hydroxide by dissolution of portlandite. In IPC there is no replenishment; the time to corrosion will depend on the ionic permeability of the paste.

in place of pure OPC, in which high-Ca/Si ratio C–S–H can play a similar role), IPC does not contain observable portlandite, even when relatively calcium-rich materials such as GGBS are present [11,31–32]. Furthermore, given the much lower solubility of calcium silicates and aluminosilicates relative to calcium hydroxide, it is clear that silicate-containing species would precipitate well before the calcium concentration was sufficient to result in precipitation of portlandite. One possible exception to this would be in hydroxide-activated IPCs synthesised from precursors with readily available Ca, in which it is possible that $Ca(OH)_2$ solubility could be exceeded, and nucleation thus takes place, before sufficient silica has been released from the solid precursor to enable formation of silicate solids. Such a mechanism has recently been hypothesised to be responsible for the formation of very localised (<100 nm) high-Ca regions within the binder phase of hydroxide-activated but not silicate-activated IPCs [33], but these cannot be observed by X-ray diffraction analysis. However, the concentration of such particulate regions (and if they are in fact $Ca(OH)_2$ rather than another calcium compound, which has not been confirmed up to this point [33]) would not be sufficiently high to introduce a significant buffering effect into the system.

Thus, unlike Portland cement, IPC has no reservoir from which to replenish the pore solution as alkali is removed. Whether or not this is of consequence to the durability of steel-reinforced inorganic polymer concretes will depend on the rate at which alkali is able to diffuse through the pore system of the paste and out of the concrete. With sufficiently low permeability, alkalinity could be maintained well beyond the anticipated life of the structure; on the other hand, IPC with low resistance to diffusion could suffer disastrous loss of alkalinity relatively rapidly. This is demonstrated schematically in Fig. 2.

3.3. Diffusion in the IPC pore system

Given the degree of porosity that is observed in IPC (Table 3; [9]), it is apparent that the alkali present in the pore solution could be leached from the paste. In the absence of a reservoir of portlandite or any similar soluble alkaline salt, this could result in a decrease in pH and depassivation of embedded steel. The extent to which this may be a problem is governed primarily by the rate at which alkali is able to diffuse through the pore system. Given a sufficiently dense and impermeable matrix, alkali leaching may not be a problem within the lifetime of a structure; on the other hand, a poorly designed IPC mix may be expected to suffer from rapid loss of alkali and subsequent loss of performance as embedded steel corrodes.

This problem is, in many ways, similar to the depassivation of reinforcing steel caused by the ingress of chloride ions. In both cases ions diffuse through the cement paste (or through the interfacial transition zone of concrete [34]) until a threshold level is reached, after which corrosion will commence. In the case of chloride attack, diffusion is inwards from an external source, while in the case of alkali in IPC the migration is outwards. Although in both cases the anion is the species of interest (Cl^- induces corrosion, while OH^- prevents it), the alkali must also diffuse to maintain electrical neutrality in the pore solution. More generally, aside from chemical reaction, the factors hindering the diffusion of one ion are likely to hinder the diffusion of others, so alkali diffusion is a marker for the diffusion of all ions into or out of the paste. While this will obviously not capture the effects of ion-specific binding, e.g. by formation of Friedel's salt in the case of chloride, the trends in diffusivity of alkalis and other ions are expected to be quite consistent across samples with similar chemistry.

Na^+ leaching curves for one-dimensional (epoxy-embedded disc; Fig. 1) IPC paste specimens synthesised from various binders are shown in Fig. 3.

Direct comparison of these data sets is difficult; under ideal conditions the rate of alkali release would reflect the mobility of alkali in the paste. However, as has already been demonstrated, changing the binder material affects both the pore volume (Table 3) and pore solution composition (Table 2), both of which affect the amount of alkali being released by the paste.

Diffusion of ions from the paste is governed, to a first approximation and in this case where no external electrical driving force is applied [35,36], by Fick's second law:

$$\frac{\partial C}{\partial t} = D\frac{\partial^2 C}{\partial x^2} \quad (1)$$

where C is the concentration of ions with diffusion coefficient, D, as a function of distance, x, at any time, t. Numerous solutions have been developed for this equation, using boundary conditions appropriate to various geometries, initial and final conditions, and so on [37]. A solution fitting the experimental conditions and geometry employed

Table 3
Porosities of IPC pastes with mix designs as outlined in the discussion of Table 2. Porosity was determined gravimetrically by calculating the difference in mass between as-cured (pores filled with water) and fully dried samples. All standard deviations are less than 5% (average of three replicate samples). Data from [9].

	Sample	Porosity (volume fraction)
Binder type	GFA	0.305
	PAFA	0.318
	HFA	0.298
	25% GGBS/75% GFA	0.330
	50% GGBS/50% GFA	0.306
	GGBS	0.269
Water/binder ratio	0.275	0.278
	0.325	0.305
	0.375	0.369
Silicate content (% by mass binder)	4	0.313
	7	0.305
	10	0.327
Na_2O content (% by mass binder)	3	0.354
	7	0.305
	11	0.303
	15	0.299
Alkali type	Na	0.305
	50:50 Na:K	0.358
	K	0.360

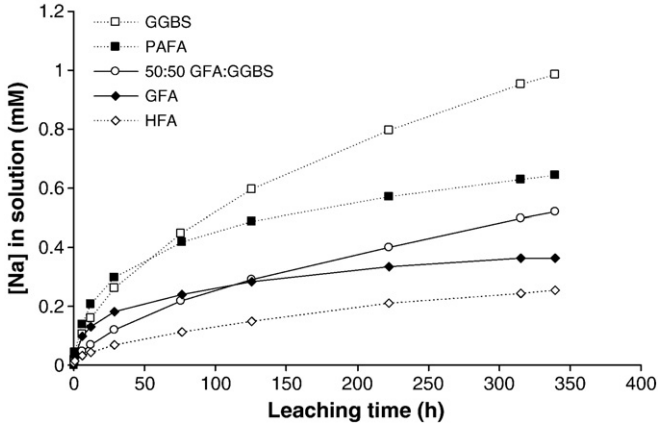

Fig. 3. Na concentration observed during RO water leaching of IPC paste synthesised from various binder materials, all with 7% Na_2O and 7% SiO_2 in the activating solution and w/b = 0.325, except GGBS with w/b = 0.350.

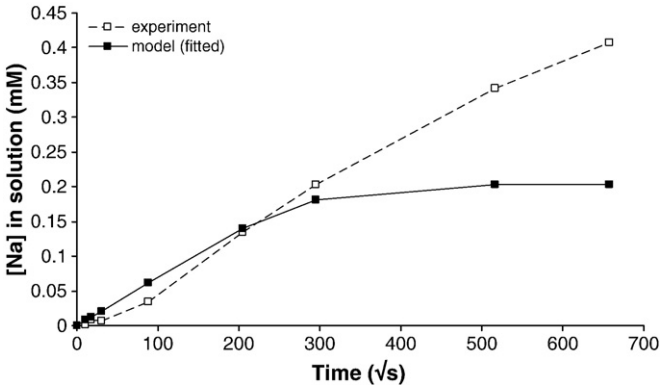

Fig. 5. Sodium leaching from GFA paste (7% Na_2O, 7% SiO_2, w/b = 0.325), showing the measured sodium concentration in leaching solution (□) and the fitted diffusion model (■), obtained by minimising the sum of squared residuals. The value of D_{eff} obtained was 4.8×10^{-11} m^2/s, using $[Na^+_0]$ = 612 mM which was measured in the expressed pore solution. Time is plotted in √s to better display the data at small values of time.

here was developed by Dorner and Beddoe [38] for diffusion of ions from cement paste:

$$\left[Na^+(t)\right] = \frac{P\left[Na_0^+\right]}{\left(P + \frac{4v}{\pi d^2 l}\right)}\left(1 - \sum_{n=1,3,5,\ldots}^{\infty} \frac{4}{\pi^2 n^2}(1-\cos(\pi n))\exp\left(-\frac{\pi^2 n^2}{l^2}D_{\text{eff}}t\right)\right) \quad (2)$$

where $[Na^+_0]$ is the initial sodium concentration in the pore solution, P is the volume fraction of porosity in the paste, v the volume of leaching solution in contact with the paste, and d and l are the diameter and thickness of the disc of paste.

All parameters required for Eq. (2), except D_{eff}, were measured directly. A Microsoft Excel spreadsheet was used to calculate values of $[Na^+(t)]$, with the summation performed up to $n = 5001$, and D_{eff} for each sample was fitted to the experimental data by minimising the sum of squared residuals using the Excel Solver functionality. There was an excellent fit between model and experimental data in many cases, as exemplified by HFA paste in Fig. 4.

However, in some cases the correlations obtained were poor, as shown in Fig. 5. In these cases the amount of sodium measured in the expressed pore solution was insufficient to account for the amount of sodium leached from the paste. Given the inherent difficulty in expressing pore solution, the possibility of Na^+ leaching from the solid binder via ion exchange or other mechanisms, the potential for error from inhomogeneous distribution of pores and other possible sources of uncertainty, the initial pore solution sodium concentration is considered the weakest piece of data input into Eq. (2). In particular, the possibility of release of bound alkalis from the aluminosilicate gel into the pores as leaching progresses cannot be discounted. This weakness is compounded by the lack of replicates; in comparison, each leaching curve consists of ten or more datum points, reducing the effect of random error.

Because of the poor fit obtained in some cases the fitting procedure was repeated, allowing both $[Na^+_0]$ and D_{eff} to vary, subject to the constraint that $[Na^+_0]$ be less than the sodium ion concentration in the activating solution used for IPC synthesis. This greatly improved the correlation between model and experiment, as shown in Fig. 6.

The value of D_{eff} obtained by using the measured value of $[Na^+_0]$ (Fig. 5) was larger by a factor of 6 than that obtained when $[Na^+_0]$ was allowed to vary (Fig. 6). The fit was clearly better when $[Na^+_0]$ was allowed to vary, however the large discrepancy between the values warranted further examination. To examine this further a comparison was made between two samples of different thickness, cut from the same specimen of paste. The parameters obtained by curve fitting are shown in Table 4.

For both data sets in Table 4, the fit obtained using the value of $[Na^+_0]$ obtained from the expressed pore solution (612 mM) was poor. When both D_{eff} and $[Na^+_0]$ were allowed to vary, however, remarkably good agreement was obtained for both values. This lends significant credence to the possibility that the alkali concentrations measured by pore solution expression are either imprecise or not fully representative of all the leachable alkalis in the IPC, and that fitting both parameters

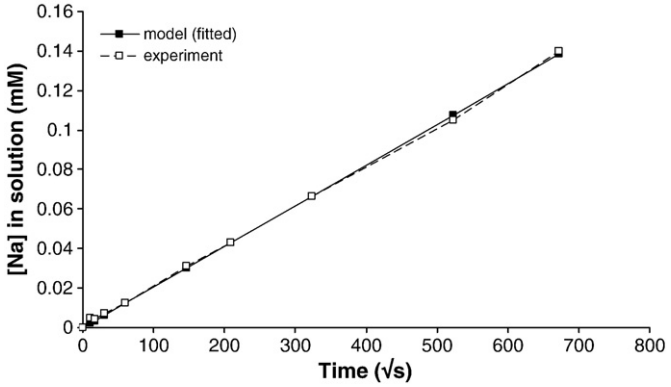

Fig. 4. Sodium leaching from HFA paste (7% Na_2O, 7% SiO_2, w/b = 0.325), showing the measured sodium concentration in leaching solution (□) and the fitted diffusion model (■), obtained by minimising the sum of squared residuals. The value of D_{eff} obtained was 6.7×10^{-13} m^2/s. Time is plotted in √s to better display the data at small values of time.

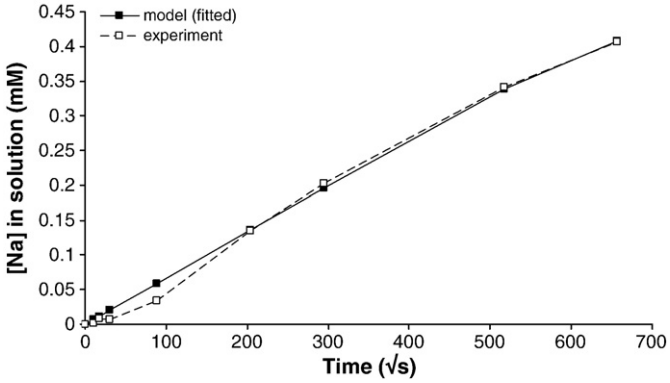

Fig. 6. Sodium leaching from GFA paste (7% Na_2O, 7% SiO_2, w/b = 0.325), showing the measured sodium concentration in the leaching solution (□) and the fitted diffusion model (■). The value of D_{eff} obtained was 7.3×10^{-12} m^2/s and $[Na^+_0]$ was 1505 mM. Time is plotted in √s to better display the data at small values of time.

Table 4
Parameters extracted from leaching data for replicate experiments using different disc thicknesses (3 mm, 5 mm) of GFA paste (7% Na_2O, 7% SiO_2, w/b = 0.325).

Disc thickness (mm)	Fixed $[Na^+_0] = 612$ mM		Optimised $[Na^+_0]$		
	D_{eff} (10^{-12} m^2/s)	R^2	$[Na^+_0]$ (mM)	D_{eff} (10^{-12} m^2/s)	R^2
3	47	0.613	1319	7.3	0.992
5	48	0.688	1505	7.3	0.996

simultaneously results in a more accurate value for D_{eff}. The repeatability of the data also demonstrates that the preparation routine followed was successful in avoiding significant modification of the surface of the sample, which might be expected to affect results obtained from relatively thin sections.

The parameters determined by fitting Eq. (2) to the alkali leaching data, allowing both D_{eff} and $[Na^+_0]$ to vary, are thus presented in Table 5. In all cases excellent correlation was achieved between the experimental data and the model. However, the absolute accuracy of these data are unknown, as this is the first study to attempt to determine diffusion coefficients for alkali leaching from IPC paste.

The D_{eff} values presented in Table 5 are many orders of magnitude higher than those determined by Muntingh [39] for chloride migration in IPC, determined using accelerated migration tests, which were reported to range from 10^{-15} to 10^{-18} m^2/s but also displayed a high degree of experimental uncertainty. Those values are in turn many orders of magnitude lower than those typical of Portland cement, and thus must be regarded with caution. In light of the high ionic strength of IPC pore solution, the use of migration tests, where an electric field gradient is used to drive ionic movement rather than diffusion, may have caused the discrepancy between accepted values for Portland cement and those of Muntingh [39].

The values presented in Table 5 are, however, similar to the chloride ion diffusion coefficients typically reported for Portland cement. For instance, Chiang and Yang [40] obtained values between 1×10^{-12} m^2/s and 6×10^{-12} m^2/s for chloride diffusion in Portland concrete. It should be noted that the results presented here are for pastes rather than concretes, and that the test applied, while fundamentally sound, has not been validated against other methods (primarily because none have yet been applied to IPC). Despite these caveats, the results presented here provide an initial estimate of the values expected. In essence, when exposed to water the alkali will diffuse from IPC approximately as quickly as chlorides diffuse into Portland concrete.

Table 5
Sample parameters determined by fitting the diffusion model to alkali leaching data for various IPC pastes. Both D_{eff} and $[Na^+_0]$ were optimised during the fitting procedure. The values of $[Na^+_0]$ determined from expressed pore solution are provided for comparison. All values of D_{eff} were obtained at 23 °C. Data for the control sample (GFA 3 mm disc, water/binder 0.325, 7% SiO_2, 7% Na_2O) are shaded in grey, as in Table 2.

Series	Sample	D_{eff} (10^{-12} m^2/s)	$[Na^+_0]$ (mM)	$[Na^+_0]$ (meas.) (mM)	R^2
Binder type	GFA (3 mm disc)	7.3	1318	612	0.992
	GFA (5 mm disc)	7.3	1505	612	0.996
	PAFA (3 mm)	6.9	1978	782	0.998
	PAFA (5 mm)	6.7	1949	782	0.994
	HFA	0.67	1567	1567	0.999
	25% GGBS	0.51	1954	711	0.993
	50% GGBS (3mm)	0.77	2327	973	0.994
	50% GGBS (5mm)	0.70	2194	973	0.999
	GGBS	0.76	6562	3617	0.994
Water/binder ratio	0.275	4.7	1169	655	0.998
	0.325	7.3	1318	612	0.992
	0.375	27	821	446	1.000
Silicate content	4%	15	4346	1227	0.993
(% by mass binder)	7%	7.3	1318	612	0.992
	10%	8.8	774	451	0.998
Na_2O content	3%	11	1715	658	0.996
(% by mass binder)	7%	7.3	1318	612	0.992
	11%	0.62	3322	1184	0.999
	15%	0.44	5084	1499	0.998
Na_2O content	7%	2.5	1059	217	0.999
(% by mass binder)	11%	1.4	2564	348	0.999
No soluble silicate	15%	2.3	5439	2069	0.999
100 m quartz	None	7.3	1318	612	0.992
aggregate	50 wt%	6.1	2032	546	0.998

3.4. Influence of IPC synthesis parameters

The composition of the binder clearly has an important effect on the diffusion of alkali from IPC paste. In particular, the presence of calcium has a dramatic effect. Binders containing significant levels of calcium (*i.e.* HFA, GGBS and GFA/GGBS blends) appear to have approximately 10-fold lower effective diffusion coefficients than their lower-Ca counterparts. This is highly significant for maintaining alkalinity at the surface of reinforcement. It is likely that the formation of calcium-containing hydrates is responsible for the decreased ionic permeability of pastes synthesised from calcium-containing raw materials.

It is well known from Portland cement chemistry that the formation of calcium silicate and aluminosilicate hydrates is accompanied by an increase in volume with respect to the anhydrous phases, thus decreasing the pore volume available for diffusion. In addition, the higher reactivity of the calcium-rich glass in GGBS relative to the aluminosilicate glass in fly ash results in a higher degree of reaction, and thus a more refined and tortuous pore system, which would also hinder the movement of ions through the paste. While there is not a great deal of difference in the absolute porosity data reported in Table 3 — and certainly not enough to explain a 10-fold difference in effective diffusion coefficients — pore refinement and tortuosity effects as highlighted in [9] are expected to contribute significantly to this reduction. This benefit would be increased by the generally higher pore solution alkalinity observed when calcium is present. Thus, using raw materials rich in calcium increases the pore solution alkalinity and decreases the rate at which alkali can leach from the pore solution, improving the likelihood that embedded reinforcement will be protected.

A reduction in the water content of the IPC mix reduces the rate of sodium diffusion, due to the lower volume of porosity and thus constriction of the pore system. The increase in diffusion coefficient observed at higher water content (w/b = 0.375) is large relative to other effects, consistent with the marked increase in porosity observed when increasing w/b to this level [9]. With an increase in porosity, and particularly in the content of larger pores, the rate of diffusion would be expected to increase dramatically.

Increasing the alkali content of the activating solution from 7% to 11% decreases the effective diffusion coefficient by a factor of 10; beyond this only a modest increase was observed. These data can be explained by the higher degree of reaction and thus pore refinement which takes place as the alkali content of the paste is increased [9]. Increasing the alkali content beyond that at which the majority of the reactive phases in the fly ash are converted to gel would provide little additional benefit.

Binders produced without soluble silicate in the activating solution showed relatively consistent effective diffusion coefficients regardless of alkali content; this indicates that the maximum extent of conversion of ash to binding phases is attained at 7% added Na_2O, at least for the curing conditions employed. At higher alkali content these binders demonstrate significantly higher ionic permeability than comparable samples produced with dissolved silica in the activating solution. This correlates well with the microstructural differences observed previously [10,18], in particular with the growth of reaction products

outwards from the surface of ash particles, leaving large interstitial voids not apparent in silicate-activated samples.

It is well known that the service life of steel-reinforced Portland concrete is significantly curtailed when exposed to chlorides [41], and the same may be expected of IPC exposed to any conditions which may cause loss of alkalinity from the paste. As the total ionic flux of alkali from IPC to initiate corrosion may be significantly different from that of chloride into Portland concrete, and because corrosion is known (to a first approximation [42]) to depend not only on the chloride concentration but also on the Cl^-/OH^- ratio [41], it is not certain for how long steel-reinforced IPC structures would be able to resist corrosion. Further modelling of the pore solution, and particularly its alkalinity, is recommended to estimate the minimum cover required for a given service life of IPC with embedded steel reinforcement. Until further studies have been completed, and the potential for corrosion of reinforcement through alkali loss better quantified, supplementary protection from corrosion should be considered for IPC concrete. Although expensive, stainless steel reinforcement may be beneficial, at least until corrosion has been more thoroughly explored.

4. Conclusions

The alkalinity of the pore solution of IPC pastes was determined directly after high pressure pore fluid expression. The values obtained indicated that the pore solution is sufficiently alkaline to passivate embedded steel. The ability of the paste to retain alkali was identified as a potential problem for IPC exposed to water, and a procedure developed to examine leaching of alkali from the paste. The results obtained indicated that alkali is highly mobile in the pore system of IPC, and that retention of alkali may significantly limit the durability of IPC with embedded steel reinforcement. The formulation of IPC played an important role in limiting alkali diffusion in the paste; in particular, the presence of calcium was important for reducing alkali mobility. Having identified alkali loss as a potentially limiting factor for the adoption of IPC, further work to refine the test methods used is warranted. Durability modelling to estimate the necessary cover over reinforcing steel is strongly recommended before IPC is used in reinforced structures. However, it does appear that it will be difficult to synthesise a durable steel-reinforced concrete within the realm of traditional aluminosilicate low-Ca 'geopolymer' compositions; the presence of calcium seems necessary for durability.

Acknowledgements

This work was funded by the Australian Research Council (ARC), including partial funding via the Particulate Fluids Processing Centre, a Special Research Centre of the ARC. We also thank Dr. A. Fernández-Jiménez for providing a prepublication copy of reference 8.

References

[1] S. Ahmad, Reinforcement corrosion in concrete structures, its monitoring and service life prediction — a review, Cem. Concr. Compos. 23 (2003) 459–471.
[2] D.W. Hobbs, Concrete deterioration: causes, diagnosis, and minimising risk, Int. Mater. Rev. 46 (3) (2001) 117–144.
[3] J. Davidovits, Geopolymers — inorganic polymeric new materials, J. Therm. Anal. 37 (8) (1991) 1633–1656.
[4] P. Duxson, A. Fernández-Jiménez, J.L. Provis, G.C. Lukey, A. Palomo, J.S.J. van Deventer, Geopolymer technology: the current state of the art, J. Mater. Sci. 42 (2007) 2917–2933.
[5] P. Duxson, J.L. Provis, G.C. Lukey, J.S.J. van Deventer, The role of inorganic polymer technology in the development of 'green concrete', Cem. Concr. Res. 37 (12) (2007) 1590–1597.
[6] J.M. Miranda, A. Fernández-Jiménez, J.A. González, A. Palomo, Corrosion resistance in activated fly ash mortars, Cem. Concr. Res. 35 (2005) 1210–1217.
[7] D. Bastidas, A. Fernández-Jiménez, A. Palomo, J.A. González, A study on the passive state stability of steel embedded in activated fly ash mortars, Corros. Sci. 50 (4) (2008) 1058–1065.
[8] A. Fernández-Jiménez, J.M. Miranda, J.A. González, A. Palomo, Steel passive state stability in activated fly ash mortars, Mater. Constr. (in press), doi:10.3989/mc.2010.53909.
[9] R.R. Lloyd, J.L. Provis, K.J. Smeaton, J.S.J. van Deventer, Spatial distribution of pores in fly ash-based inorganic polymer gels visualised by Wood's metal intrusion, Microporous Mesoporous Mater. 126 (1–2) (2009) 32–39.
[10] R.R. Lloyd, J.L. Provis, J.S.J. van Deventer, Microscopy and microanalysis of inorganic polymer cements. 1. Remnant fly ash particles, J. Mater. Sci. 44 (2) (2009) 608–619.
[11] R.R. Lloyd, Ph.D. Thesis, University of Melbourne, Australia, 2008.
[12] R.S. Barneyback, S. Diamond, Expression and analysis of pore fluids from hardened cement pastes and mortars, Cem. Concr. Res. 11 (1981) 279–285.
[13] D. Rothstein, J.J. Thomas, B.J. Christensen, H.M. Jennings, Solubility behavior of Ca-, S-, Al-, and Si-bearing solid phases in Portland cement pore solutions as a function of hydration time, Cem. Concr. Res. 32 (2002) 1663–1671.
[14] J.J. Thomas, D. Rothstein, H.M. Jennings, B.J. Christensen, Effect of hydration temperature on the solubility behaviour of Ca-, S-, Al-, and Si-bearing solid phases in Portland cement pastes, Cem. Concr. Res. 33 (2003) 2037–2047.
[15] P. Duxson, G.C. Lukey, F. Separovic, J.S.J. van Deventer, The effect of alkali cations on aluminum incorporation in geopolymeric gels, Ind. Eng. Chem. Res. 44 (4) (2005) 832–839.
[16] P. Duxson, J.L. Provis, G.C. Lukey, J.S.J. van Deventer, F. Separovic, Z.H. Gan, ^{39}K NMR of free potassium in geopolymers, Ind. Eng. Chem. Res. 45 (26) (2006) 9208–9210.
[17] S.-Y. Hong, F.P. Glasser, Alkali sorption by C–S–H and C–A–S–H gels: part II. Role of alumina, Cem. Concr. Res. 32 (7) (2002) 1101–1111.
[18] R.R. Lloyd, J.L. Provis, J.S.J. van Deventer, Microscopy and microanalysis of inorganic polymer cements. 2. The gel binder, J. Mater. Sci. 44 (2) (2009) 620–631.
[19] S.-D. Wang, K.L. Scrivener, Hydration products of alkali activated slag cement, Cem. Concr. Res. 25 (1995) 561–571.
[20] I.G. Richardson, A.R. Brough, G.W. Groves, C.M. Dobson, The characterization of hardened alkali-activated blast-furnace slag pastes and the nature of the calcium silicate hydrate (C–S–H) paste, Cem. Concr. Res. 24 (5) (1994) 813–829.
[21] B. Lothenbach, A. Gruskovnjak, Hydration of alkali-activated slag: thermodynamic modelling, Adv. Cem. Res 19 (2) (2007) 81–92.
[22] F. Puertas, A. Fernández-Jiménez, M.T. Blanco-Varela, Pore solution in alkali-activated slag cement pastes. Relation to the composition and structure of calcium silicate hydrate, Cem. Concr. Res. 34 (2004) 139–148.
[23] P. Faucon, T. Charpentier, A. Nonat, J.C. Petit, Triple-quantum two-dimensional ^{27}Al magic angle nuclear magnetic resonance study of the aluminum incorporation in calcium silicate hydrates, J. Am. Chem. Soc. 120 (46) (1998) 12075–12082.
[24] S. Song, H.M. Jennings, Pore solution chemistry of alkali-activated ground granulated blast-furnace slag, Cem. Concr. Res. 29 (1999) 159–170.
[25] A. Gruskovnjak, B. Lothenbach, L. Holzer, R. Figi, F. Winnefeld, Hydration of alkali-activated slag: comparison with ordinary Portland cement, Adv. Cem. Res 18 (3) (2006) 119–128.
[26] P. Duxson, G.C. Lukey, F. Separovic, J.S.J. van Deventer, Effect of alkali cations on aluminum incorporation in geopolymeric gels, Ind. Eng. Chem. Res. 44 (2005) 832–839.
[27] P. Duxson, S.W. Mallicoat, G.C. Lukey, W.M. Kriven, J.S.J. van Deventer, The effect of alkali and Si/Al ratio on the development of mechanical properties of metakaolin-based geopolymers, Colloids Surf., A 292 (2007) 8–20.
[28] P. Duxson, J.L. Provis, G.C. Lukey, J.S.J. van Deventer, F. Separovic, Z.H. Gan, ^{39}K NMR of free potassium in geopolymers, Ind. Eng. Chem. Res. 45 (2006) 9208–9210.
[29] M. Criado, A. Fernández-Jiménez, A.G. de la Torre, M.A.G. Aranda, A. Palomo, An XRD study of the effect of the SiO_2/Na_2O ratio on the alkali activation of fly ash, Cem. Concr. Res. 37 (2007) 671–679.
[30] I. Soroka, Portland Cement Paste and Concrete, Macmillan, London, 1979 338 pp.
[31] L.M. Keyte, Ph.D. Thesis, University of Melbourne, Australia, 2008.
[32] C.A. Rees, J.L. Provis, G.C. Lukey, J.S.J. van Deventer, Attenuated total reflectance Fourier transform infrared analysis of fly ash geopolymer gel ageing, Langmuir 23 (15) (2007) 8170–8179.
[33] J.L. Provis, V. Rose, S.A. Bernal, J.S.J. van Deventer, High resolution nanoprobe X-ray fluorescence characterization of heterogeneous calcium and heavy metal distributions in alkali activated fly ash, Langmuir 25 (19) (2009) 11897–11904.
[34] C.C. Yang, Effect of the percolated interfacial transition zone on the chloride migration coefficient of cement-based materials, Mater. Chem. Phys. 91 (2005) 538–544.
[35] E. Samson, J. Marchand, K.A. Snyder, Calculation of ionic diffusion coefficients on the basis of migration test results, Mater. Struct. 36 (2003) 156–165.
[36] L. Tang, J. Gulikers, On the mathematics of time-dependent apparent chloride diffusion coefficient in concrete, Cem. Concr. Res. 37 (2007) 589–595.
[37] J. Crank, The Mathematics of Diffusion, 2nd Ed.Clarendon Press, Oxford, 1975 414 pp.
[38] H.W. Dorner, R.E. Beddoe, Prognosis of concrete corrosion due to acid attack, 9th International Conference on Durability of Materials and Components, Brisbane, Australia, 17–21 March 2002, CD-ROM Proceedings, 2002, (Ed.), pp.
[39] Y. Muntingh, M.Sc. Thesis, University of Stellenbosch, South Africa, 2006.
[40] C.T. Chiang, C.C. Yang, Relation between the diffusion characteristic of concrete from salt ponding test and accelerated chloride migration test, Mater. Chem. Phys. 106 (2007) 240–246.
[41] F.P. Glasser, J. Marchand, E. Samson, Durability of concrete — degradation phenomena involving detrimental chemical reactions, Cem. Concr. Res. 38 (2) (2008) 226–246.
[42] K. Sagoe-Crentsil, F.P. Glasser, "Green rust", iron solubility and the role of chloride in the corrosion of steel at high pH, Cem. Concr. Res. 23 (1993) 785–791.